Uncertainty Bounds for State Estimates with Applications in Target Tracking

James C. Spall[1]

The Johns Hopkins University, Applied Physics Laboratory, Laurel, MD, 20723, USA

Shihong Wei[2]

Department of Applied Mathematics and Statistics, Johns Hopkins University, Baltimore, MD, 21218, USA

Abstract. **This work considers the application of the extended Kalman filter (EKF) in systems with nonlinear state transition equations. We develop a surrogate-based method to approximate the uncertainty bounds of the EKF using only one trajectory, without the need to simulate many independent replicates. This method is demonstrated in a target tracking problem in 3D space.**

I. Introduction

Estimating locations and trajectories of mobile targets is a problem of key interest in many defense systems. Typically, a target can only be partially observed via sensor or radar systems. As an aid in target tracking, state-space models are built to describe both the motion of the target and the sensing process. Furthermore, filtering (state estimation) algorithms such as the Kalman filter and its many variants have long been used to recover real-time kinematic information on the state of the target from the noisy sensor measurements collected to the current time point. Target tracking using the state estimation framework has been widely applied in many defense and non-defense settings, such as monitoring the motion of unmanned aerial vehicles (UAV), detecting illegal border-crossings, and conducting the mission of battlefield surveillance (see ref. [1] for some examples and discussion). That said, little is known about the statistical properties of the error in the state estimate in the presence of nonlinearities in the state-space model and/or non-normality of the random noises. In this paper, we present a method of calculating probabilistic bounds for the state estimation error in nonlinear target tracking systems when some popular recursive filters, such as the constant gain Kalman filter (CGKF) and extended Kalman filter (EKF), are applied.

Characterizing the uncertainty of the state estimation error is important and beneficial in several respects: First, it demonstrates how well the target state and its trajectory is being monitored and managed via the state estimation process. Second, probabilistic bounds for the tracking error transfer

[1]Principal Professional Staff, Applied Physics Laboratory, 11100 Johns Hopkins Road, Laurel, MD 20723, USA (james.spall@jhuapl.edu).

[2]Department of Applied Mathematics and Statistics, 3400 North Charles Street, Baltimore, MD, 21218, USA (swei15@jhu.edu).

AIAA Defense Forum, 11–13 April 2023

naturally to simultaneous confidence intervals (regions) of the target. Then, it becomes possible to evaluate the probability of a moving target showing up in a specified region. Third, knowledge about the tracking error facilitates the design and the comparison of efficient estimation algorithms and sensor systems. Fourth, a proper characterization of the filter error may also be useful in calculating uncertainty bounds for parameter estimates in system identification (see, e.g., [2] and [3], for aerospace examples).

Despite the importance of determining statistical bounds for the estimation error in the CGKF and EKF, the problem remains largely unsolved, especially when the system is nonlinear. The technical challenges are multifold. It is well-known that even a Gaussian random quantity is not guaranteed to stay in the same distributional family after a nonlinear transformation. Because of the iterated nonlinear transformations and non-decaying noises in the system across time points, the distribution of the target estimate and its error are usually unknowable, and there is no guarantee that they will be a named distribution such as Gaussian. In fact, even for linear systems where a Kalman filter is applied, the error distribution is generally non-Gaussian when all or some of the noise terms in the state equation or measurement equation are non-Gaussian. Moreover, as shown in refs. [4] and [5], the distribution remains unknown even in large samples (i.e., there is no central limit effect). In particular, it has been observed that the most recent noise terms have a larger impact on the error distribution than earlier noise terms. Hence, the use of central limit theorem is, in general, invalid to obtain an approximate probability distribution for the error in the asymptotic case. In addition, for the reasons above, the commonly assumed $N(\mathbf{0}, \boldsymbol{P})$ distribution for the error, where $\boldsymbol{P}$ is the EKF analogue to the classical error-covariance matrix in a linear filter, is also flawed.

Refs. [6] and [7] demonstrate the same principle of non-Gaussian state error in scalar nonlinear systems. Although for some continuous systems, a Fokker-Planck equation can be built to describe the transition of the distribution of the state estimation error in dynamical systems (see ref. [8]), there exists no closed-form solution for the desired distribution. Finally, probability bounds such as the Chebyshev inequality can sometimes be used to construct conservative confidence regions, but those regions are often too large to be of practical value. Without knowledge of the probability distribution of the filtering error, calculating uncertainty bounds can be very difficult. In this paper, we provide a means for a rigorous and practical way to determine the uncertainty bounds (confidence regions) of the estimation error in the EKF, and illustrate its application in a target-tracking problem.

II. Motivating Application

While the method here is generic and applicable to a broad class of nonlinear systems, we will illustrate the method via a target tracking problem. In this work, a discrete-time state-space model modified from Sect. 6.3.3 in [9] is used to represent the target tracking problem with nonlinear acceleration. In particular, let us consider the case when the dynamics of acceleration are controlled by a nonlinear mapping, which models the situation where the motion of a target is "smoothly" maneuvered. This is a generalization of the popular constant velocity motion model used in [10], the constant acceleration motion model used in [11], or the nearly constant acceleration motion model used in [12]. Allowing the acceleration to change smoothly, the velocity and the trajectory of the target will have more flexibility compared with the classic constant acceleration motion model.

For the measurement system, it is assumed in this paper that the target can only be partially observed via a linear mapping with noise. For example, consider the case when the height of the target is unavailable, but the information about the latitude and the longitude is available, or only the latitude is

observed. Another example is tracking or surveilling objects within a fixed camera's view so that the received information is projected to a 2D screen.

To estimate the true state of the target from noisy observations in a tracking setting, nonlinear recursive filters are applied (see ref. [13] for an example). That is, a target motion model and an observation model are constructed to reflect the dynamics in the true physical process of the target motion and the data acquisition. Given the previous target state estimate, the one-step ahead prediction and the expected observation are computed according to the system model. Once the newest measurement is observed, the residual (difference between the observed data and the expected observation) can be calculated. Integrating the one-step-ahead prediction and the information in the residual, the target state estimate is updated to the current time step. The illustrative application of thise paper is the tracking error, i.e., the difference between the true target state and the filtering estimate. A schematic of this state estimation process when the target is a UAV drone is given in Figure 1.

In this paper, our analysis will focus on the situation when the generic EKF or CGKF is used in the tracking problem. As one of the most popular nonlinear filtering algorithms, the EKF is widely used in the field of target tracking and collision avoidance (see ref. [14] for an example). Meanwhile, although the CGKF, as a constant-gain tracker, is not as adaptive as varying-gain algorithms such as the EKF, it provides considerable computational savings when the dimension of the problem is high or when there is a need for rapid data processing. Applications of constant-gain target trackers can be found in problems like aircraft engine performance estimation [15], wireless sensor networks [16], and prediction of reentry of risk objects [17].

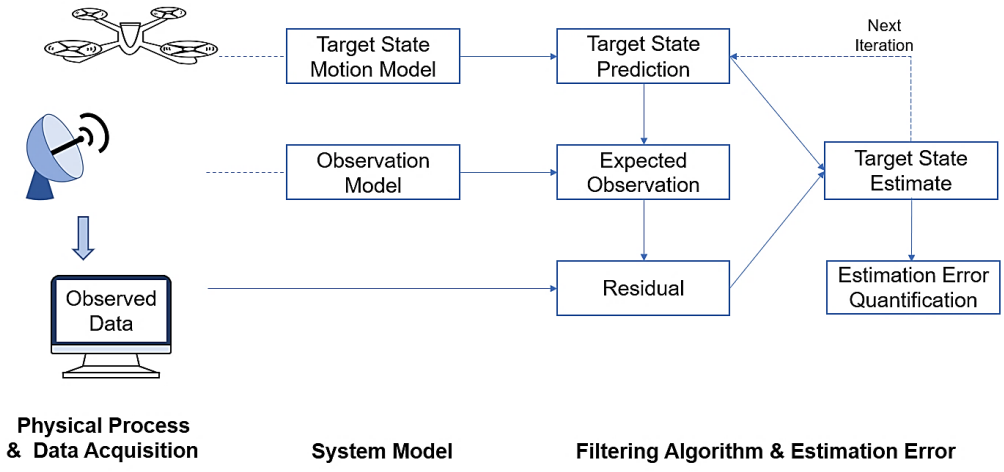

Figure 1. Schematic of the target tracking problem. A UAV drone is the target.

For linear systems with symmetric noise distributions and with the Kalman filter used for the state estimation, it was shown in [5] that a surrogate process can be constructed that stochastically dominates the unknown distribution of the tracking error. Then, the confidence regions of the surrogate will automatically serve as the approximate confidence regions for the true error. In scalar nonlinear systems with either the extended Kalman filter or the constant-gain filter, a similar analysis is presented in [6]. However, for nonlinear systems, the error distribution is not guaranteed to be symmetric or well-shaped, so its confidence region can be ill-shaped. Consequently, it is not possible to use the same arguments as

[5] or [6] to create a surrogate with the appropriate stochastic dominance relationships in the multivariate nonlinear case.

III. Overview of Analytical Approach and Extensions

A. State-Space Model and EKF

Given a time sampling interval ΔT, the discrete-time state-space model below is taken as the mathematical representation of the evolution of the unknown target state $\boldsymbol{x}_k$ and the associated measurement process:

$$\boldsymbol{x}_k = \boldsymbol{f}(\boldsymbol{x}_{k-1}) + \boldsymbol{w}_k$$
$$\boldsymbol{z}_k = \boldsymbol{H}\boldsymbol{x}_k + \boldsymbol{v}_k,$$

where $\boldsymbol{f}$ is a (generally) nonlinear state transformation function, $\boldsymbol{H}$ is a linear measurement matrix, and $\boldsymbol{z}_k$ is the observed information at the time step k. Moreover, we assume that the noise terms $\boldsymbol{w}_k$ in the state transformation equation and $\boldsymbol{v}_k$ in the measurement equation have mean zero and finite magnitude covariance matrices. We further assume that the noise terms themselves are both independent and identically distributed random variables, and that $\boldsymbol{w}_k$ and $\boldsymbol{v}_k$ are independent.

Then, given a trajectory of the noisy observations $\boldsymbol{z}_{1,\dots,}\boldsymbol{z}_k$, the EKF algorithm (ref. [18, Sect. 13.2]) generates the state estimate $\widehat{\boldsymbol{x}}_k$ of the unknown target state $\boldsymbol{x}_k$ recursively by $\widehat{\boldsymbol{x}}_k = \boldsymbol{f}(\widehat{\boldsymbol{x}}_{k-1}) + \boldsymbol{K}_k[\boldsymbol{z}_k - \boldsymbol{H}\boldsymbol{f}(\widehat{\boldsymbol{x}}_{k-1})]$, where $\boldsymbol{K}_k$ is the EKF gain matrix computed at the time step k. Meanwhile, a matrix $\boldsymbol{P}_k$ (sometimes erroneously called an error-covariance matrix) is computed in the algorithm iterations to update the EKF gain matrix. Then, our goal in this work is to develop robust and effective methods to compute the confidence intervals (regions) for the state estimation error of the EKF defined as:

$$\boldsymbol{e}_k = \boldsymbol{x}_k - \widehat{\boldsymbol{x}}_k.$$

B. Motivation and Background

To calculate uncertainty bounds for the unknown distribution of the tracking error, a surrogate process is constructed in a manner different from the method for linear systems in [5]. Under certain conditions, it can be shown that the generalized method here provides an appropriate surrogate probability distribution for nonlinear systems that is close to the unknown distribution for the true error; see ref. [19] for analysis when the Kalman-like gain matrix (traditionally called $\boldsymbol{K}_k$, as shown in Sect. III.A) is decaying to $\mathbf{0}$ across iterations ($k \to \infty$). Therefore, their regions of high confidence (probability) are close, so we can use the confidence regions of the surrogate as the approximate confidence regions for the actual tracking error. The approach is expected to be applicable for all common distributions of additive system noises with finite second moment, such as Gaussian or *t*-distribution. The methods of ref. [19], however, are inappropriate in a target tracking setting because tracking is not possible with a gain matrix decaying to $\mathbf{0}$. Therefore, we need a new method applicable in the setting of a non-decaying gain matrix.

As above, the estimation error is defined as the difference between the true state and the filter estimate. To develop a new surrogate process that is applicable for tracking problems, we need to develop a method that does not require that the gain matrix decays to $\mathbf{0}$. We first apply the multivariate mean value theorem, leading to an error term that is an autoregressive (AR) process with random and dependent coefficient matrices. We use ergodicity theory to construct another surrogate AR process with

deterministic coefficients estimated from the ergodic averages, i.e., averages over one trajectory. The characteristic functions of both the true error and the surrogate are analyzed to investigate how close their distributions are. Under some conditions, an upper-bound is derived for the distance between two distributions for each component of the error and the surrogate. Therefore, the probability that the surrogate falls into a specified confidence region is close to the probability that the tracking error falls into the region, so it is possible to calculate approximate uncertainty bounds for the error and eventually for the target state. An illustration of the analytical approach is shown in Figure 2.

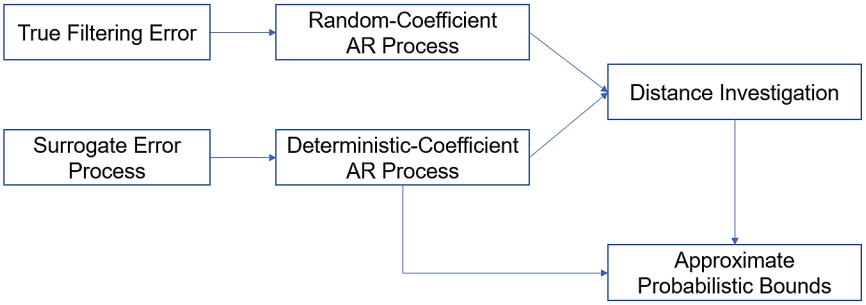

Figure 2. Illustration of the analytical approach.

For example, if a valid Gaussian surrogate is constructed, the approximate uncertainty regions for the unknown tracking error will be hyper-ellipsoids. Consequently, we can calculate approximate confidence regions of the target as hyper-ellipsoids centered at the current state estimate point.

The framework and the analysis in this work can also be extended to systems with nonlinear measurement transformations or other variants of Kalman filters, as long as the ergodicity of the system can be established (i.e., the system is able to reach a stochastic steady state). In that way, the method here has potential in tracking problems as well as other DoD-related problems where it is important to have some clear understanding of how close the state estimate is to the unknown true state.

C. Method Description

Given that the aforementioned state transformation function $\boldsymbol{f}$ is twice continuously differentiable, we can express the error dynamic in the following AR form:

$$\begin{aligned} \boldsymbol{e}_{k+1} &= (\boldsymbol{I}-\boldsymbol{K}_{k+1}\boldsymbol{H})[\boldsymbol{f}(\boldsymbol{x}_k)-\boldsymbol{f}(\hat{\boldsymbol{x}}_k)+\boldsymbol{w}_{k+1}]-\boldsymbol{K}_{k+1}\boldsymbol{v}_{k+1} \\ &\equiv (\boldsymbol{I}-\boldsymbol{K}_{k+1}\boldsymbol{H})\boldsymbol{F}_{k+1}\boldsymbol{e}_k+[(\boldsymbol{I}-\boldsymbol{K}_{k+1}\boldsymbol{H})\boldsymbol{w}_{k+1}-\boldsymbol{K}_{k+1}\boldsymbol{v}_{k+1}] \\ &\equiv \boldsymbol{B}_k\boldsymbol{e}_k+\boldsymbol{\varepsilon}_{k+1}. \end{aligned}$$

where $\boldsymbol{F}_{k+1}$ is based on the first-order approximation inherent in the EKF. However, $\boldsymbol{F}_{k+1}$ is not computable since (from the mean-value theorem of calculus) each row is evaluated at a point between $\hat{\boldsymbol{x}}_k$ and the unknown true $\boldsymbol{x}_k$. Note that $\boldsymbol{e}_n=\sum_{k=0}^{n}\boldsymbol{B}_{nk}\boldsymbol{\varepsilon}_k$ with $\boldsymbol{B}_{nk}=\prod_{i=k}^{n-1}\boldsymbol{B}_i$ for $k<n$, and $\boldsymbol{B}_{nn}=\boldsymbol{I}$.

As shown above, the error dynamics can be expressed as a multivariate AR process with random (probabilistically) dependent coefficients $\boldsymbol{B}_k$ that can not be computed directly as well as dependent noise terms $\boldsymbol{\varepsilon}_k$ (due to the random EKF gain matrix $\boldsymbol{K}_k$ being sequentially dependent in general). Consequently, there are several technical challenges in computing its confidence regions. First, the exact distribution of $\boldsymbol{e}_k$ is usually unknown due to the iterated nonlinear transformation and persistent noises. Even asymptotically, there is, in general, no central limit effect to guarantee a normally

distributed error (see [4] and [5] for details in the linear case; [6] or [7] for the nonlinear case). Second, despite the common assumption that $\boldsymbol{P}_k$ in the EKF represents the error-covariance matrix $(\mathrm{cov}(\boldsymbol{e}_k))$ (e.g. pp. 399 and 402 in [18]), the matrix $\boldsymbol{P}_k$ may, in fact, be a poor estimate of $\mathrm{cov}(\boldsymbol{e}_k)$. (A dramatic example of this phenomenon was shown in the oral presentation slides associated with this paper at the AIAA Defense Forum in April 2023; the true 95% confidence interval in the example was over 10 times wider than the interval predicted by the use of the commonly assumed $N(\mathbf{0}, \boldsymbol{P}_k)$ distribution.)

In order to address the challenges above, we propose a surrogate-based approximation method similar to the constant-gain Kalman filter case in [20]. Specifically, we construct a surrogate process $\bar{\boldsymbol{e}}_n$ whose distribution is close to the unknown true error distribution $\boldsymbol{e}_n$ under certain conditions. Meanwhile, the surrogate distribution itself must be computable or be easily simulated. As we assume only one trajectory of observations $\boldsymbol{z}_1, \dots, \boldsymbol{z}_n$, note that the EKF error $\boldsymbol{e}_k, k = 1, 2, \dots, n,$ demonstrates a "settling down" or ergodic behavior for large *n* in some systems. To construct a surrogate process that mimics the true error dynamics $\boldsymbol{e}_k$ as closely as possible, let us use the following AR surrogate process $\bar{\boldsymbol{e}}_k$:

$$\bar{\boldsymbol{e}}_{k+1} = \boldsymbol{C}_k \bar{\boldsymbol{e}}_k + \boldsymbol{\eta}_{k+1},$$

with $\boldsymbol{C}_k$ being a particular deterministic matrix and $\boldsymbol{\eta}_{k+1}$ being an appropriate noise term.

First, if the system settles down after some transient phase, we expect that the Kalman gain will also settle down, and we can approximate its value by some ergodic average (one-path average of dependent terms). Consequently, we replace $\boldsymbol{\varepsilon}_k$ with $\boldsymbol{\eta}_k$ having the same distribution as $(\boldsymbol{I} - \boldsymbol{K}^*\boldsymbol{H})\boldsymbol{w}_k - \boldsymbol{K}^*\boldsymbol{v}_k$, where $\boldsymbol{K}^*$ is the limiting value of $\bar{\boldsymbol{K}}_n = \sum_{k=1}^{n} \boldsymbol{K}_k/n$. Second, since $\boldsymbol{B}_k$ is not directly observable or easily computable, we replace it with a computable quantity related to the Jacobian matrix. Specifically, we use $\boldsymbol{C}_k \equiv (\boldsymbol{I} - \boldsymbol{K}^*\boldsymbol{H})\boldsymbol{J}^*$, where $\boldsymbol{J}^*$ is the limiting (ergodic) average from $\bar{\boldsymbol{J}}_n = \sum_{k=1}^{n} \boldsymbol{J}_k/n,$ and $\boldsymbol{J}_k$ is the Jacobian (matrix derivative) of $\boldsymbol{f}$ evaluated at $\hat{\boldsymbol{x}}_k$ for $k = 1, \cdots, n$. Note that both $\boldsymbol{J}_k$ and $\boldsymbol{F}_k$ are from the first-order approximation but that only $\boldsymbol{J}_k$ is computable since it is evaluated at a known point. Therefore, the surrogate process $\bar{\boldsymbol{e}}_k$ is an AR process with deterministic coefficients and independent noise terms, so its limiting or finite-sample distribution can be potentially computed. In practice, we use the observed quantities $\bar{\boldsymbol{K}}_n$ and $\bar{\boldsymbol{J}}_n$ for large values of *n* as approximations to the limiting values $\boldsymbol{K}^*$ and $\boldsymbol{J}^*$. Using theory of Markov processes, the formal justification for the approach above is given in [20] for the CGKF case; the corresponding justification in the EKF case is ongoing research, but a numerical demonstration of the validity is given in Sect. IV below.

Note that in the important special case where the initial state and noise terms in the state-space model are all Gaussian distributed, then the limiting distribution for $\bar{\boldsymbol{e}}_n$ is $N(\mathbf{0}, \overline{\boldsymbol{P}})$, where $\overline{\boldsymbol{P}} = \lim_{n\to\infty} \mathrm{cov}(\bar{\boldsymbol{e}}_n)$. We can approximate $\overline{\boldsymbol{P}}$, the limiting surrogate covariance matrix by running *n* iterations of the recursion $\mathrm{cov}(\bar{\boldsymbol{e}}_{k+1}) = \boldsymbol{C}_k \mathrm{cov}(\bar{\boldsymbol{e}}_k)\boldsymbol{C}_k^T + \mathrm{cov}(\boldsymbol{\eta}_{k+1})$. Note that $\boldsymbol{J}^*$ and $\boldsymbol{K}^*$, as needed in the recursion, are approximated by ergodic average values from a large number of iterations (which is available). This approach based on $N(\mathbf{0}, \overline{\boldsymbol{P}})$ is used in the calculation of probabilities and confidence regions in Section IV below.

IV. Numerical Study

A. Kinematic State-Space Model

The following numerical study example is based on Section III and the kinematic models described in [10] and [11]. Consider a maneuvering object in the *xyz* plane (3-dimensional space), and the EKF is

used to track the kinematic state of the target. At each time step, the target state is described as the following 9×1 vector:

$$\boldsymbol{x} = \left[p_x, v_x, a_x, p_y, v_y, a_y, p_z, v_z, a_z\right]^T,$$

where p_x, p_y and p_z denote the position of the target along axis x, y and z, respectively. Furthermore, v_x, v_y and v_z denote the corresponding velocities, and a_x, a_y and a_z denote the corresponding accelerations. A graphical illustration of the tracking problem is given in Figure 3.

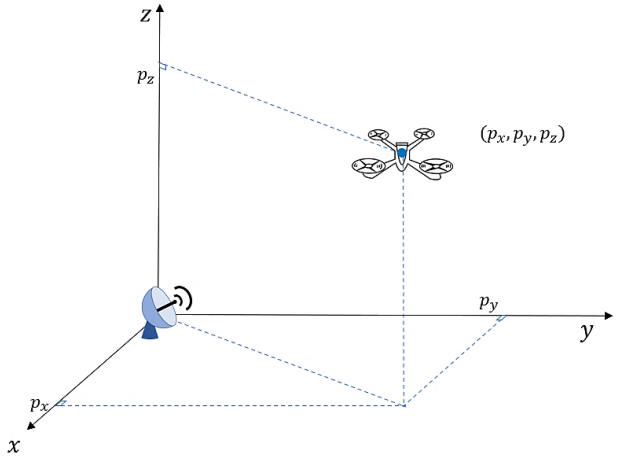

Figure 3. Graphical illustration of the target tracking problem.

We follow the notation in the standard state-space model in Sect. III.A. Following ref. [9, Chap. 6], we choose a specific form of the state transition function by setting $\boldsymbol{f}(\boldsymbol{x}) = \boldsymbol{A}\boldsymbol{x} + \boldsymbol{u}(\boldsymbol{x})$, where the 9×9 matrix $\boldsymbol{A}$ is taken as a block diagonal matrix with each of the three 3×3 blocks in $\boldsymbol{A}$ being

$$\begin{bmatrix} 1 & \Delta T & \frac{\Delta T^2}{2} \\ 0 & 0 & \Delta T \\ 0 & 0 & 1 \end{bmatrix},$$

and the control function $\boldsymbol{u}$ is as follows:

$$\boldsymbol{u}(\boldsymbol{x}_k) = \begin{bmatrix} -0.1\boldsymbol{x}_{k1} \\ -0.1\boldsymbol{x}_{k2} \\ -0.5\boldsymbol{x}_{k3} + 0.5\sin(\boldsymbol{x}_{k3}) \\ -0.05\boldsymbol{x}_{k4} \\ -0.05\boldsymbol{x}_{k5} \\ -0.5\boldsymbol{x}_{k6} + 0.5\cos(\boldsymbol{x}_{k6}) \\ -0.05\boldsymbol{x}_{k7} \\ -0.05\boldsymbol{x}_{k8} \\ -0.5\boldsymbol{x}_{k9} + 0.5\sin(\boldsymbol{x}_{k9}) \end{bmatrix}.$$

The covariance matrix $\boldsymbol{Q}$ of the state noise $\boldsymbol{w}_k$ is taken as a block diagonal matrix with each of the three 3×3 blocks being:

$$\sigma_w^2 \begin{bmatrix} \frac{\Delta T^4}{4} & \frac{\Delta T^3}{2} & \frac{\Delta T^2}{2} \\ \frac{\Delta T^3}{2} & \Delta T^2 & \Delta T \\ \frac{\Delta T^2}{2} & \Delta T & 1 \end{bmatrix}.$$

For the measurement model, we assume that the state can be partially observed through the measurement matrix $\boldsymbol{H}$ below and the measurements have additive noise $\boldsymbol{v}_k$ with a covariance matrix as follows:

$$\boldsymbol{H} = \begin{bmatrix} 1 & 0 & 0 & 0 & 0 & 0 & 0 & 0 & 0 \\ 0 & 0 & 0 & 1 & 0 & 0 & 0 & 0 & 0 \\ 0 & 0 & 0 & 0 & 0 & 0 & 1 & 0 & 0 \end{bmatrix} \text{ and } \boldsymbol{R} = \sigma_v^2 \begin{bmatrix} \Delta T & 0 & 0 \\ 0 & \Delta T & 0 \\ 0 & 0 & \Delta T \end{bmatrix}.$$

In this example, let us assume that for illustrative purpose $\Delta T = 0.05,\ \sigma_w = 4,\ \sigma_v = 2$, and all noises (and initial state) are Gaussian.

B. Statistical Justification for Use of Surrogate Method with EKF

As mentioned in Sect. III.C, the surrogate method has been formally justified in the case of the CGKF but not (yet) in the case of the EKF. However, in ongoing research, partial theoretical and statistical (numerical) justification has been completed for the EKF. We now present some of the statistical justification.

In particular, to provide partial statistical justification of the convergence of the error $\boldsymbol{e}_k$ in distribution, using the model in Sect. IV.A above, let us simulate one long trajectory of 10^5 samples of the filtering error $\boldsymbol{e}_k$. Note that convergence in distribution is a critical part of justifying the above-discussed stochastic steady-state behavior and ergodic averaging. Because the points along the same trajectory are dependent, we use the method of batch means (see ref. [21, Chap. 4]) to create nearly independent samples for use with standard statistical tests. We use a batch size of 250 and drop the first 10^4 samples for the "burn-in" (transient) period. Therefore, we have $(10^5 - 10^4)/250 = 360$ batch mean values for each of the nine components of the error.

Then, let us perform the following three statistical tests for the batch mean values. We use the following tests:

(i) Runs test for randomness (independence), where the null hypothesis is that after batch mean processing, the values are independent (see ref. [22, Sect. 4.5]).

(ii) Matched-pair *t*-test for first 180 batch mean values against the last 180 batch mean values (among the total of 360 batch means along one trajectory), where the null hypothesis is that the mean values of the two divided groups are the same (see ref. [23, Appendix B]).

(iii) Kolmogorov-Smirnov (KS) goodness-of-fit test, where the null hypothesis is that the two groups come from the same distribution.

Table 1 below shows the probability values (*P*-values) of all three tests using the batch means for each of the nine components. The results show that at the level of 0.05 for each test, the individual tests fail to reject the null hypothesis. Hence, there is no statistical indications of behavior that is contrary to that predicted by the surrogate process method. Note that because we are testing multiple hypotheses above, a multiple comparisons test (such as the Tukey-Kramer method) could also be applied (ref. [23,

Chap. 12]). However, given that there was no rejection of any null hypothesis in Table 1, and given that multiple comparisons tests widen the associated intervals for hypothesis testing, it appears that no adjustment for multiple comparisons is needed here.

Table 1. *P*-values of statistical tests applied to batch mean values.

Component of $\boldsymbol{e}_{1000}$	Runs Test	Matched-Pairs *t*-Test	KS Test
1st Component p_x	0.34	0.29	0.56
2nd Component v	1.00	0.11	0.17
3rd Component a_x	0.09	0.14	0.40
4th Component p_y	0.46	0.86	0.82
5th Component v_y	0.17	0.85	0.82
6th Component a_y	0.92	0.85	0.48
7th Component p_z	0.92	0.68	0.89
8th Component v_z	0.46	0.46	0.48
9th Component a_z	0.21	0.42	0.56

C. Numerical Results

We now apply this surrogate-based method to the 3D tracking problem described above and compute confidence intervals for each component of $\boldsymbol{e}_{1000}$. Figure 4 shows the marginal density plots of the surrogate overlaying those of the empirical terminal error density obtained from 10^4 independent replicates, where the dashed curves are the marginal density of the surrogate $\bar{\boldsymbol{e}}_{1000}$ and the red solid curves are the marginal empirical density of true $\boldsymbol{e}_{1000}$. Note that the surrogate densities are the Gaussian marginal densities derived from the $N(\mathbf{0}, \bar{\boldsymbol{P}})$ distribution, as mentioned at the end of Section III.

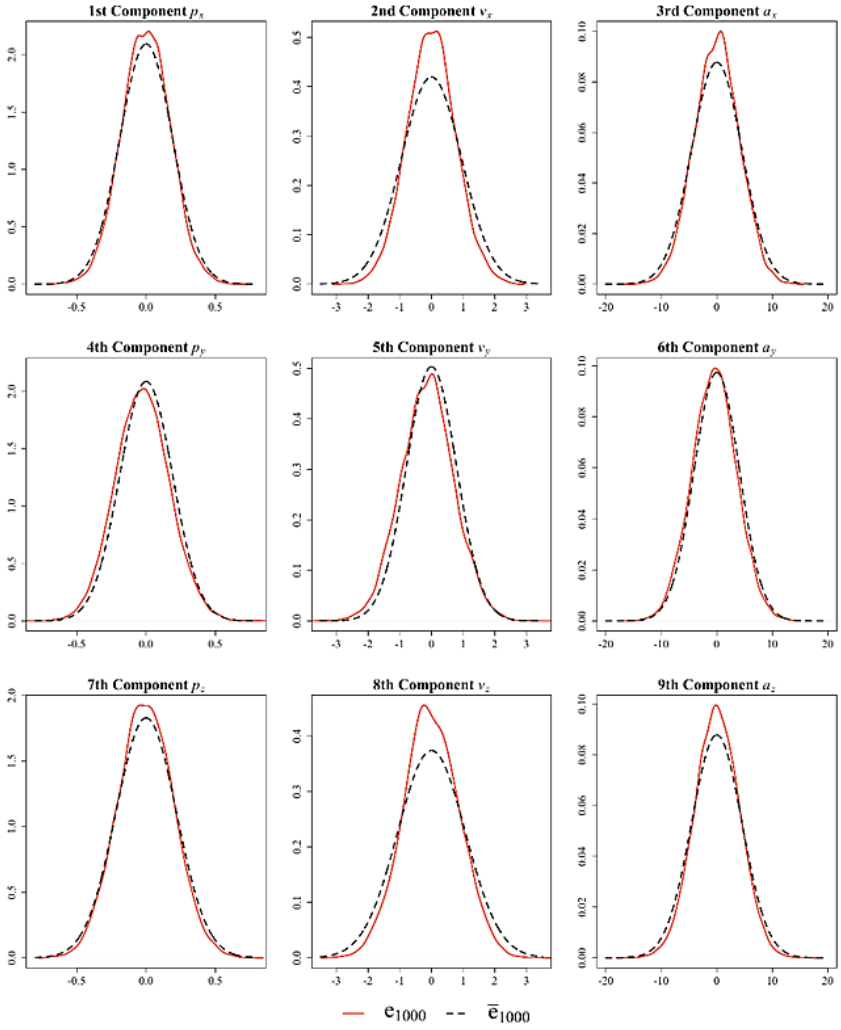

Figure 4. Marginal empirical densities of e_{1000} (solid line) vs. marginal densities of surrogate $\bar{e}_{1000}$ (dashed line).

Although there are some discrepancies between the density curves of the nine components in Figure 4, the surrogate densities computed from one trajectory are close to the corresponding empirical error density from the 10^4 independent replicates in all cases. This demonstrates the effectiveness of the surrogate as an approximation.

The 95% confidence intervals of each component of the terminal error are summarized in Table 2 below. As shown, the surrogate confidence intervals are close to the corresponding empirical quantiles of the true error. This result is in line with the density plots in Figure 4.

Table 2. 95% confidence intervals from empirical quantiles of e_{1000} and Gaussian-based quantiles for the surrogate $\bar{e}_{1000}$.

Component of e_{1000}	Empirical Quantiles	Surrogate Approximation
1st Component p_x	$(-0.344, 0.340)$	$(-0.373, 0.373)$
2nd Component v	$(-1.500, 1.535)$	$(-1.864, 1.864)$
3rd Component a_x	$(-7.871, 7.713)$	$(-8.906, 8.906)$
4th Component p_y	$(-0.403, 0.363)$	$(-0.375, 0.375)$
5th Component v_y	$(-1.745, 1.534)$	$(-1.555, 1.555)$
6th Component a_y	$(-8.303, 7.420)$	$(-8.031, 8.031)$
7th Component p_z	$(-0.395, 0.386)$	$(-0.427, 0.427)$
8th Component v_z	$(-1.734, 1.711)$	$(-2.094, 2.094)$
9th Component a_z	$(-7.897, 7.949)$	$(-8.915, 8.915)$

V. Conclusions

In this work, we consider the application of the EKF algorithm in target-tracking problems with nonlinear discrete-time systems. We introduce a surrogate-based method to approximate the uncertainty bounds for the state estimation error of the EKF error using one trajectory. The method is relatively easy to use in that it relies on simple running (ergodic) averages of certain quantities in the EKF. Ongoing work is extending the theoretical justification for the method from the CGKF setting in ref. [20] to the EKF setting. This paper provides further support for the method through numerical tests in a standard tracking setting. It is shown that the uncertainty bounds computed from the surrogate method are close to the empirical confidence bounds of the error distribution.

References

[1] A. Ez-Zaidi and S. Rakrak, "A comparative study of target tracking approaches in wireless sensor networks," *J. Sensors*, vol. 2016, 11 pages, 2016, doi: 10.1155/2016/3270659.

[2] C. Grillo and F. Montano (2015), "An extended Kalman filter-based technique for on-line identification of unmanned aerial system parameters," *Journal of Aerospace Technology and Management*, vol. 7, pp. 323–333.

[3] J. C. Spall and J. P. Garner, "Parameter identification for state-space models with nuisance parameters," *IEEE Transactions on Aerospace and Electronic Systems*, vol. 26(6), pp. 992–998, 1990.

[4] J. C. Spall and K. D. Wall, "Asymptotic distribution theory for the Kalman filter state estimator," *Commun. Stat. — Theory Methods*, vol. 13, no. 16, pp. 1981–2003, 1984, doi: 10.1080/03610928408828808.

[5] J. L. Maryak, J. C. Spall, and B. D. Heydon, "Use of the Kalman filter for inference in state-space models with unknown noise distributions," *IEEE Trans. Autom. Control*, vol. 49, no. 1, pp. 87–90, Jan. 2004, doi: 10.1109/TAC.2003.821415.

[6] S. Wei and J. C. Spall, "Uncertainty quantification for the extended and the deterministic-gain Kalman filters," in *Proceedings of 2022 American Control Conference (ACC)*, Atlanta, GA, Jun. 2022, pp. 2341–2346.

[7] S. Wei and J. C. Spall, "Probabilistic bounds for a class of filtering algorithms in the scalar case," in *Proceedings of 2021 American Control Conference (ACC)*, New Orleans, LA, May 2021, pp. 4039–4044. doi: 10.23919/ACC50511.2021.9483036.

[8] M. Kumar and S. Chakravorty, "Nonlinear filter based on the Fokker-Planck equation," *J. Guid. Control Dyn.*, vol. 35, no. 1, pp. 68–79, Jan. 2012, doi: 10.2514/1.54070.

[9] Y. Bar-Shalom, X.-R. Li, and T. Kirubarajan, *Estimation with Applications to Tracking and Navigation*. John Wiley & Sons, 2001. doi: 10.1002/0471221279.

[10] Z. Tian, K. Yang, M. Danino, Y. Bar-Shalom, and B. Milgrom, "Launch point estimation with a single passive sensor without trajectory state estimation," *IEEE Trans. Aerosp. Electron. Syst.*, vol. 58, no. 1, pp. 318–327, Feb. 2022, doi: 10.1109/TAES.2021.3098837.

[11] Z. Hou and F. Bu, "A small UAV tracking algorithm based on AIMM-UKF," *Aircr. Eng. Aerosp. Technol.*, vol. 93, no. 4, pp. 579–591, Jan. 2021, doi: 10.1108/AEAT-01-2019-0013.

[12] K. Li, Z. Guo, and G. Zhou, "Nearly constant acceleration model for state estimation in the range-Doppler plane," *IET Radar Sonar Navig.*, vol. 15, no. 12, pp. 1687–1701, 2021, doi: 10.1049/rsn2.12157.

[13] J. N. Gross, Y. Gu, M. B. Rhudy, S. Gururajan, and M. R. Napolitano, "Flight-test evaluation of sensor fusion algorithms for attitude estimation," *IEEE Trans. Aerosp. Electron. Syst.*, vol. 48, no. 3, pp. 2128–2139, Jul. 2012, doi: 10.1109/TAES.2012.6237583.

[14] Luo, S. I. McClean, G. Parr, L. Teacy, and R. De Nardi, "UAV position estimation and collision avoidance using the extended Kalman filter," *IEEE Trans. Veh. Technol.*, vol. 62, no. 6, pp. 2749–2762, Jul. 2013, doi: 10.1109/TVT.2013.2243480.

[15] T. Kobayashi, D. L. Simon, and J. S. Litt, "Application of a constant gain extended Kalman filter for in-flight estimation of aircraft engine performance parameters," in *Proceedings of the ASME Turbo Expo 2005: Power for Land, Sea, and Air.*, Reno, NV, Jun. 2005, pp. 617–628. doi: 10.1115/GT2005-68494.

[16] A. Yadav, N. Naik, M. R. Ananthasayanam, A. Gaur, and Y. N. Singh, "A constant gain Kalman filter approach to target tracking in wireless sensor networks," in *2012 IEEE 7th International Conference on Industrial and Information Systems (ICIIS)*, Aug. 2012, pp. 1–7. doi: 10.1109/ICIInfS.2012.6304803.

[17] K. Anilkumar, M. R. Ananthasayanam, and P. V. Subba Rao, "A constant gain Kalman filter approach for the prediction of re-entry of risk objects," *Acta Astronaut.*, vol. 61, no. 10, pp. 831–839, Nov. 2007, doi: 10.1016/j.actaastro.2007.01.063.

[18] D. Simon, *Optimal state estimation: Kalman, H∞, and nonlinear approaches*. John Wiley & Sons, 2006.

[19] J. L. Maryak, J. C. Spall, and G. L. Silberman, "Uncertainties for recursive estimators in nonlinear state-space models, with applications to epidemiology," *Automatica*, vol. 31, no. 12, pp. 1889–1892, Dec. 1995, doi: 10.1016/0005-1098(95)00109-9.

[20] S. Wei and J. C. Spall, "Quantifying the estimation error for a constant-gain tracker," in *Proc. American Control Conference (ACC)*, San Diego, CA, 31 May–2 June 2023.

[21] R. Y. Rubinstein and D. P. Kroese, *Simulation and the Monte Carlo Method* (3rd edition), Wiley, ISBN: 978-1-118-63216-1, 2017.

[22] P. Sprent and N. C. Smeeton, *Applied Nonparametric Statistical Methods*, CRC Press, 2007.

[23] J. C. Spall (2003), *Introduction to Stochastic Search and Optimization: Estimation, Simulation, and Control*, Wiley, Hoboken, NJ.